Rapid Scan EPR Imaging

Gareth R. Eaton, Mark Tseitlin, Tomasz Czechowski, Richard W. Quine, George A. Rinard, and Sandra S. Eaton,

Department of Chemistry and Biochemistry and Department of Engineering, University of Denver

Funding: EB002180

"Those who have the highest-resolution tools in science can ask the most important questions, and those that have such tools first can answer the important questions first. Instrumentation gives one the competitive edge and underlies almost everything that goes on in science."

-- Mark Wrighton, 2000 Ullyot lecture

Enabling Technologies

- Magnet
  - Magnetic field control
  - Magnet power supply – stability into inductive load, voltage compliance for fast field changes
  - Magnetic field gradient systems
  - Rapid magnetic field scan coils and driver
- RF/microwave source – phase noise, amplitude noise
- Resonator – Reflection, Transmission (crossed loop)
  - AFC/ACC/ATC to compensate for physiological motion
- Signal detection
  - CW, pulse, rapid scan
  - Dynamic range, bandwidth, noise sources, A/D resolution
- Samples – trityl, nitroxyl
- Software to operate spectrometer and acquire spectra
- Software to analyze spectra and images
- Image reconstruction
  - Fourier
  - Filtered back projection (FBP)
  - Maximum entropy (MEM)

Enabling Technologies

Resonators

- Reflection
- Transmission (crossed loop)

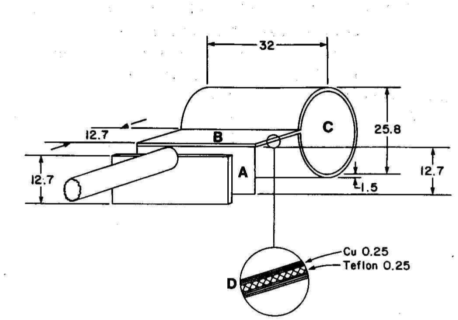

FIG. 2. Design details of the resonator (dimensions are in millimeters): (a) coupling capacitor, (b) resonator capacitor, (c) resonator inductor and sample holder, and (d) inset: detail of capacitor material.

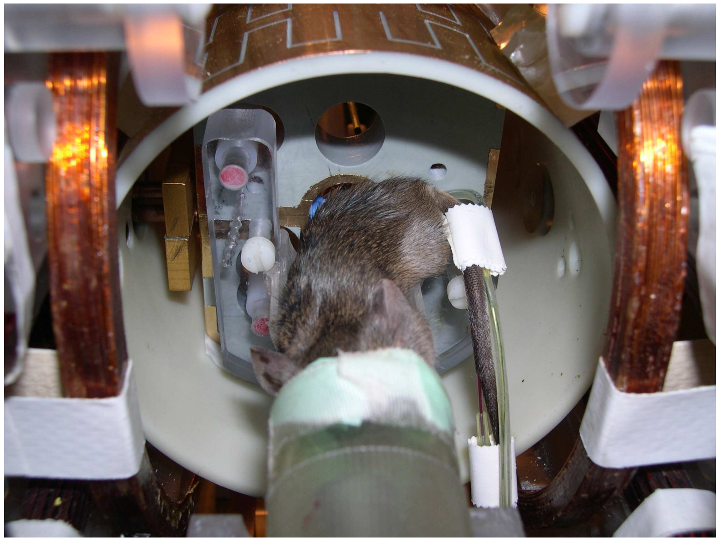

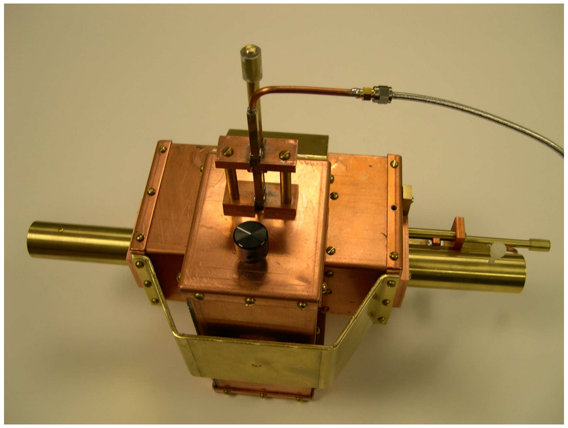

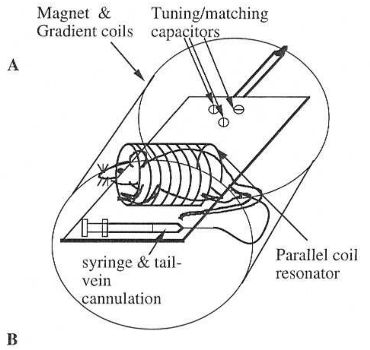

Magnets

ca.90 G (9 mT) field for 250 MHz EPR

air-core magnets for access
4-coil magnets for homogeneity

Magnetic field control
Magnet power supply
•stability into inductive load
•voltage compliance for fast field changes
Magnetic field gradient systems
Rapid magnetic field scan coils and driver

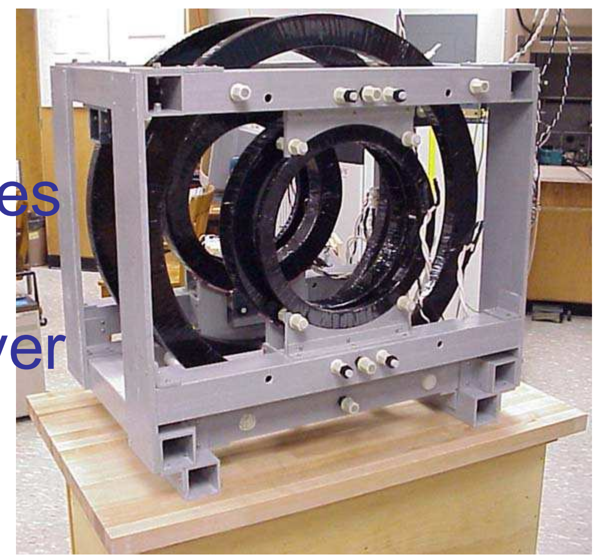

RF/microwave bridge

Source – low noise
Tuning, gain, signal path isolation
AFC/ACC/ATC to compensate for physiological motion
Signal detection – CW, pulse, rapid scan

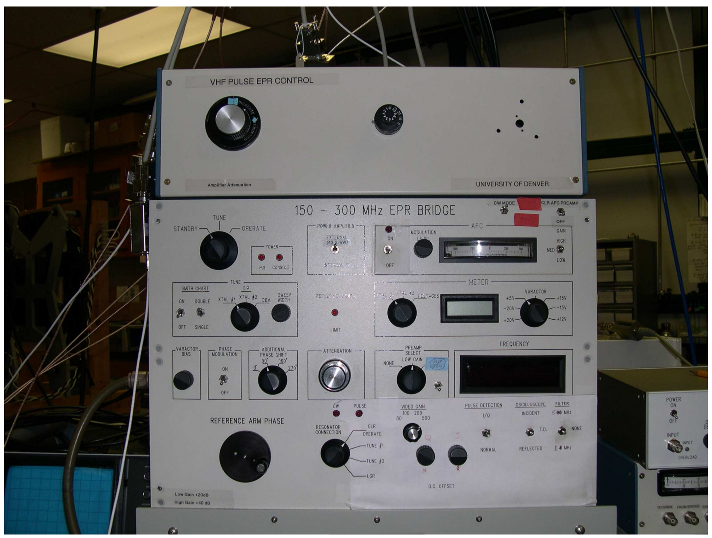

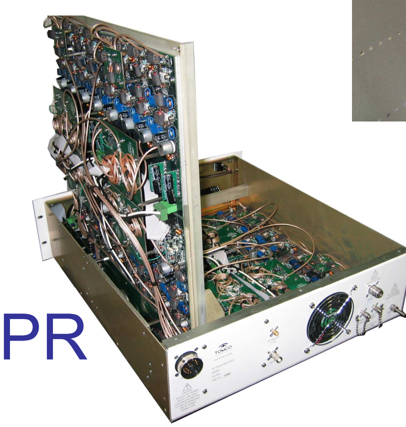

Pulse amplifier for pulsed EPR

Rapid scan EPR
a new enabling technology for in vivo imaging

- What is rapid scan EPR?
- Rapid scans of LiPc and trityl radicals
- Wider scans for nitroxyls
- Imaging

LiPc

$R = CD_3$ trityl-CD_3

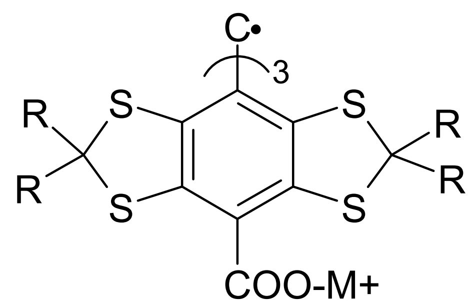

Perspective

Slow-scan – CW, linear response

↓

Rapid-scan – relaxation dependent response

↓

Time domain – pulse response

Rapid Scan Imaging

Technology is being developed to enable rapid scan imaging.

Rapid scan involves scanning the magnetic field at rates that result in relaxation-dependent EPR signal responses.

Rapid scan generates the absorption signal, which decreases in amplitude linearly with increase in gradient, not quadratically as for first derivative spectra.

This will be a major advantage for imaging.

Rapid scan coils are 4-coil air core magnets, similar to the main magnet.

Coils are shown here before final assembly.

Also shown is the green RF shield around the resonator.

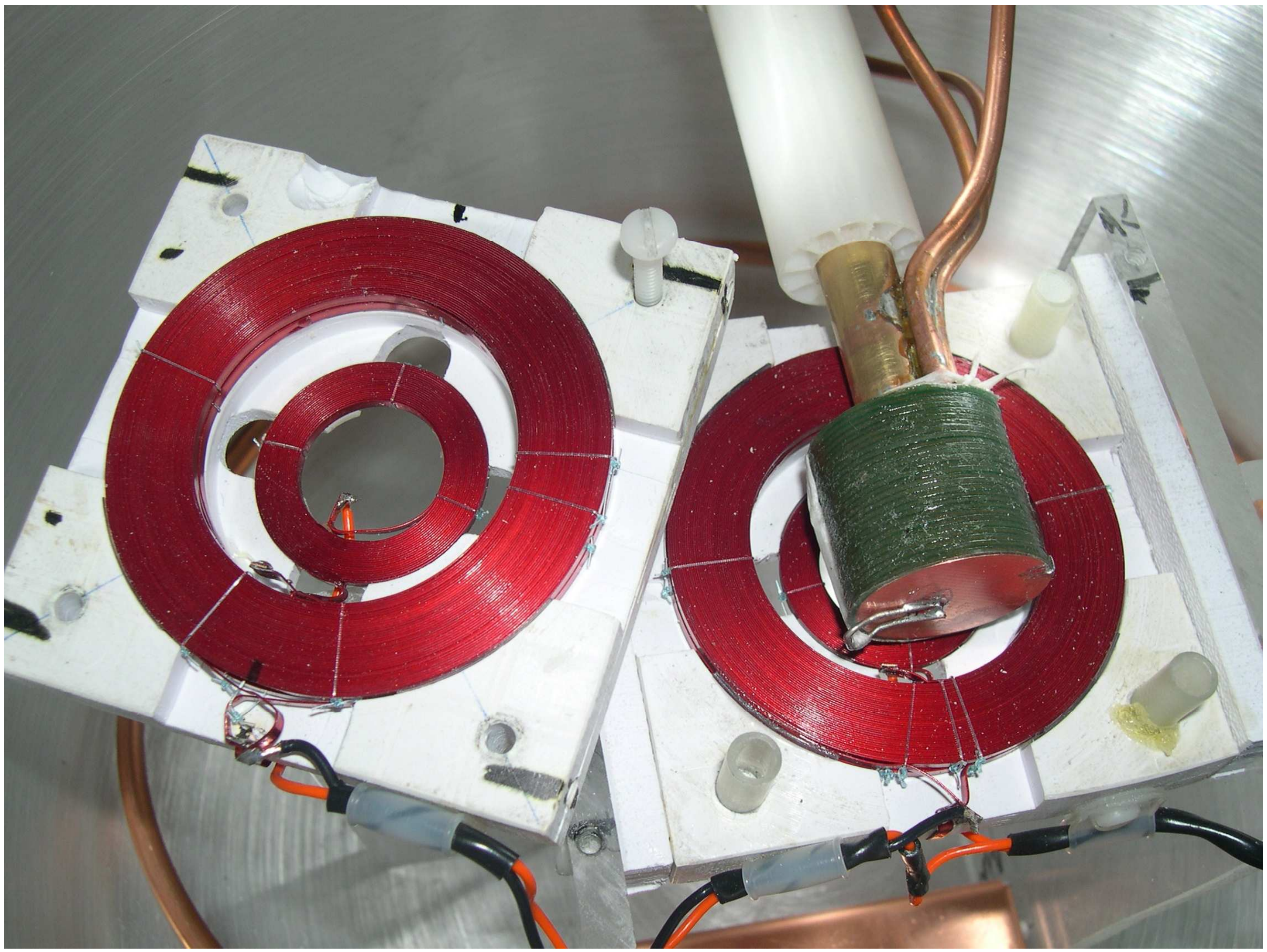

T_2 of Nitroxyl Radical Tempone-d_{16} at 245 MHz

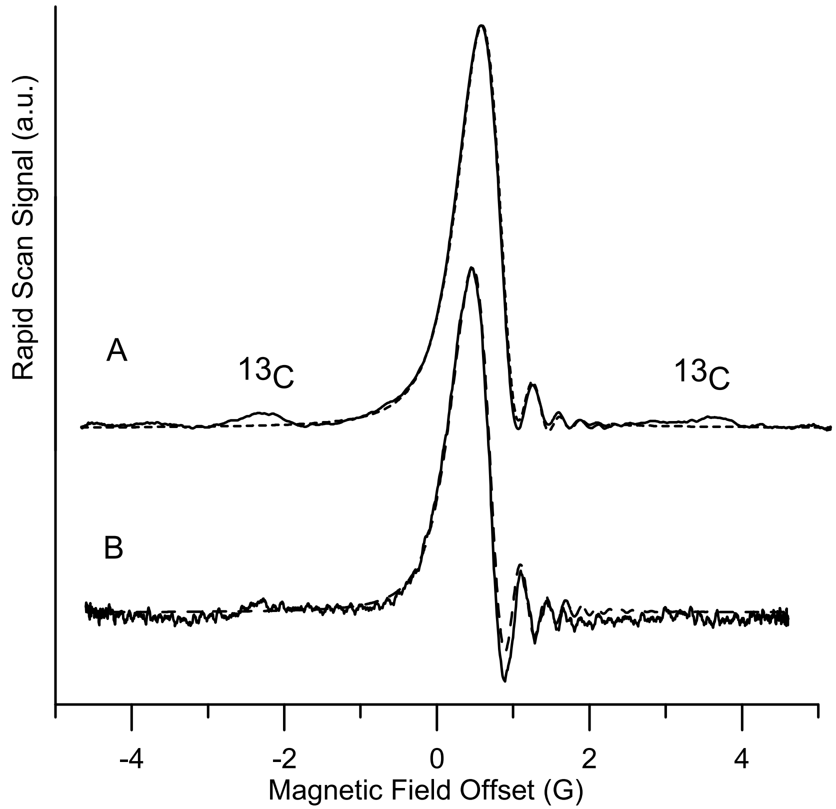

0.5 mM solution
T_2 = 0.38 μs

0.1 mM solution
T_2 = 0.56 μs

Rapid scan signals for the low-field line of tempone-d_{16} in water obtained with 40 kHz sinusoidal field sweeps.

The dashed lines are simulations.

Rapid-Scan EPR

- Rapid means that the magnetic field passes through resonance for a spin packet in a time that is short relative to the relaxation time T_2.

- Oscillations are observed on the trailing edge of the signal when

$$[\gamma(dB_o/dt)]^{0.5}\ T_2 > 1$$

- The absorption signal (not the first derivative) is detected.

- When the signal is broadened by a gradient in an imaging experiment the amplitude of the absorption signal decreases linearly, but the amplitude of the first derivative signal decreases approximately quadratically.

Simulation of Rapid Scan Signals

Simulations of the rapid scan signals were performed by numerical integration of the rotating-frame representation of the Bloch equations.

$$\frac{dM_u}{dt} = \frac{-M_u}{T_2} - (\Delta\omega + \Omega_m \,\mathrm{fscn}(\omega_m t)M_v$$

$$\frac{dM_v}{dt} = (\Delta\omega + \Omega_m \,\mathrm{fscn}(\omega_m t))M_u - \frac{M_v}{T_2} - \gamma B_1 M_z$$

$$\frac{dM_z}{dt} = \frac{M_0}{T_1} + \gamma B_1 M_v - \frac{M_z}{T_1}$$

$\Delta\omega$ is the offset of a spin packet from the center of the scan in angular units
B_1 is the RF magnetic field in Gauss
Ω_m is the magnitude of the field scan in angular units
fscn is the sinusoidal or triangular scan function

LiPc at 9.8 GHz

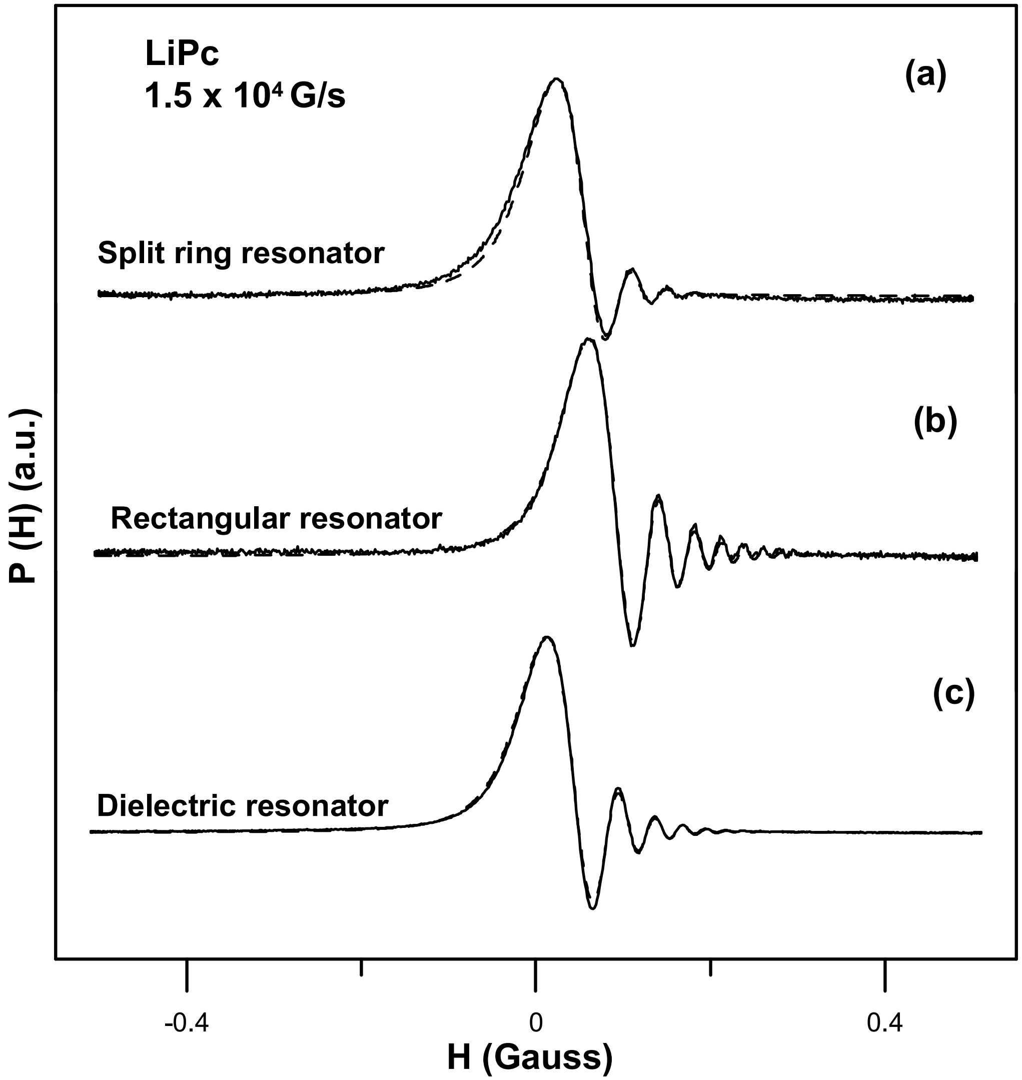

- Spectra recorded using the split-ring resonator and the dielectric resonator have larger inhomogeneous broadening than the ones recorded using the rectangular resonator.
- The inhomogeneous broadening increases with increasing scan rate. It is proposed that inhomogeneities are the result of eddy currents induced in metal components of the resonator assembly by the rapid scans.
- These spectra were obtained at scan rates slow enough that the resonator Q did not cause distortions of the time response.

Triangular Field Scans

- Our first results were obtained with sinusoidal field scans generated using the modulation driver in a Bruker console.
- In a sinusoidal scan the rate changes continuously through the spectrum. The maximum rate in the center of the scan is 2π x scan frequency x scanwidth/2.

- We have built triangular scan generators with scan frequencies between 1 and 10 kHz and scan widths of 0.5 to 50 G.
- In a triangular scan the sweep width is constant through essentially all of the scan.
- The undistorted absorption signal can be recovered from the triangular-scan rapid-scan signals by Fourier deconvolution.
- The signals from the up- and down- scans can be combined to improve signal-to-noise.

Rapid Scans at 250 MHz

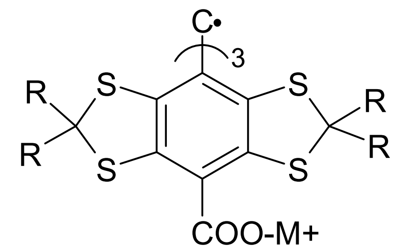

R = CD_3 trityl-CD3

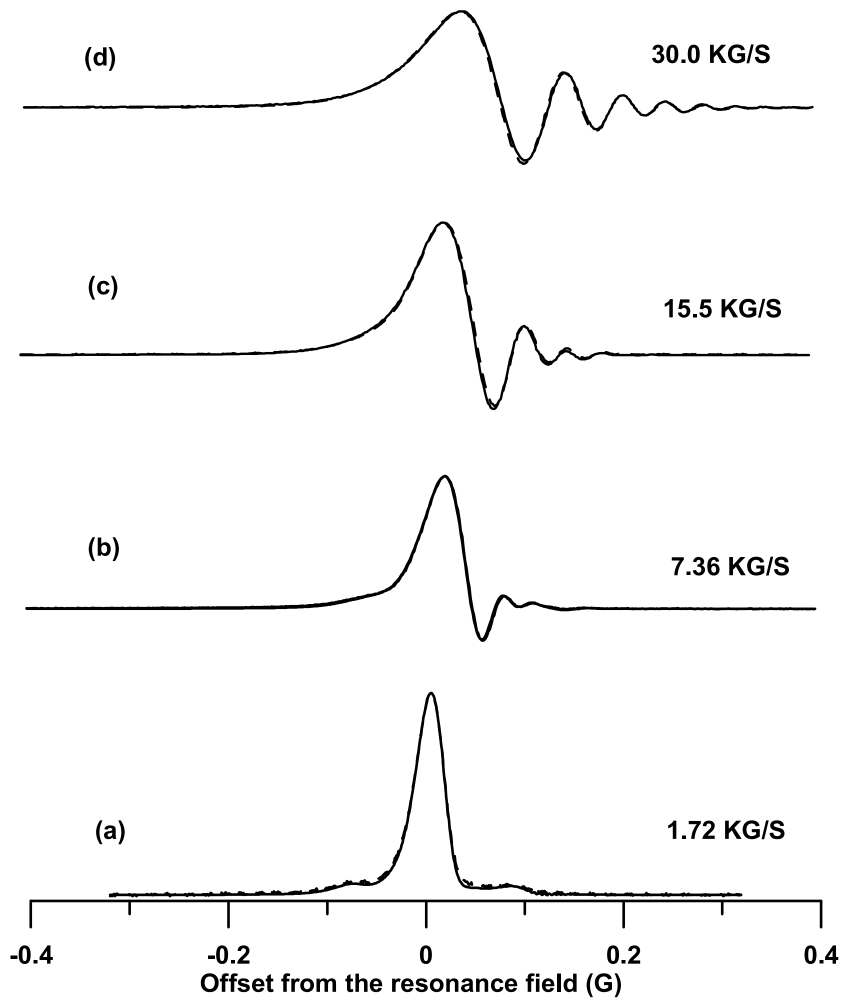

Triangular rapid-scan signals for a 0.2 mM aqueous trityl solution.

Scan rates are fast relative to the reciprocals of the relaxation times.
T_1 = 12 μs and T_2 = 11.5 μs

Solid lines are the experimental data and dashed lines are the simulations.

The scale on the x axis is the offset in Gauss from the center of the scan.

Fourier Deconvolution

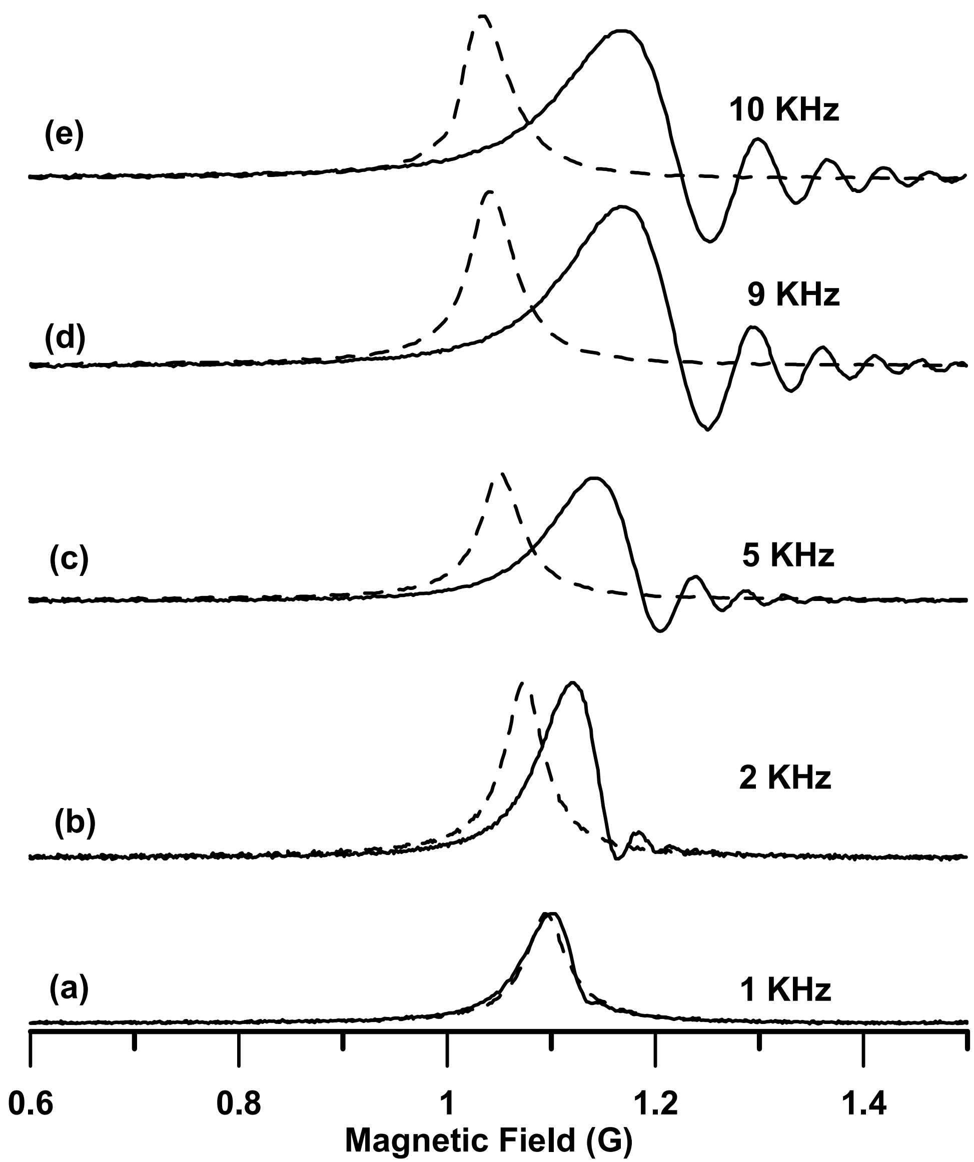

Triangular rapid-scan signals (solid lines) for a LiPc sample obtained with scan rates of (a-e) 4.32, 8.64, 21.6, 38.8, and 43.2 KG/s.

The dashed lines are the deconvolved absorption lineshapes.

LiPc Rapid Scan Signal Intensities

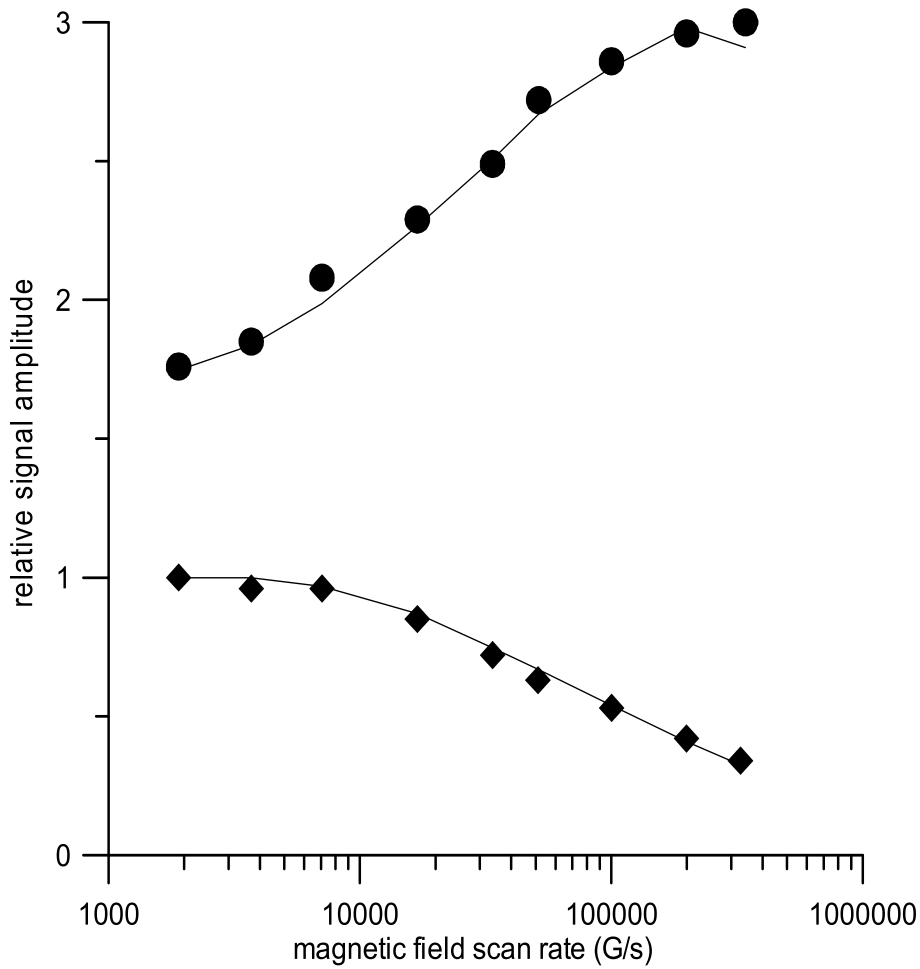

Relative intensities for the LiPc signal at the center of a sinusoidal scan as a function of scan rate at a constant RF B_1 of 6.5×10^{-3} G (♦) and at the B_1 that gave the maximum signal amplitude (•).

Relative signal amplitudes were scaled to 1.0 for the signal at constant B_1 of 6.5×10^{-3} G at a scan rate of 1.3×10^{3} G/s .

Solid lines are relative intensities calculated using numerical integration of the Bloch equations.

Impact of Gradient on Signal Amplitude

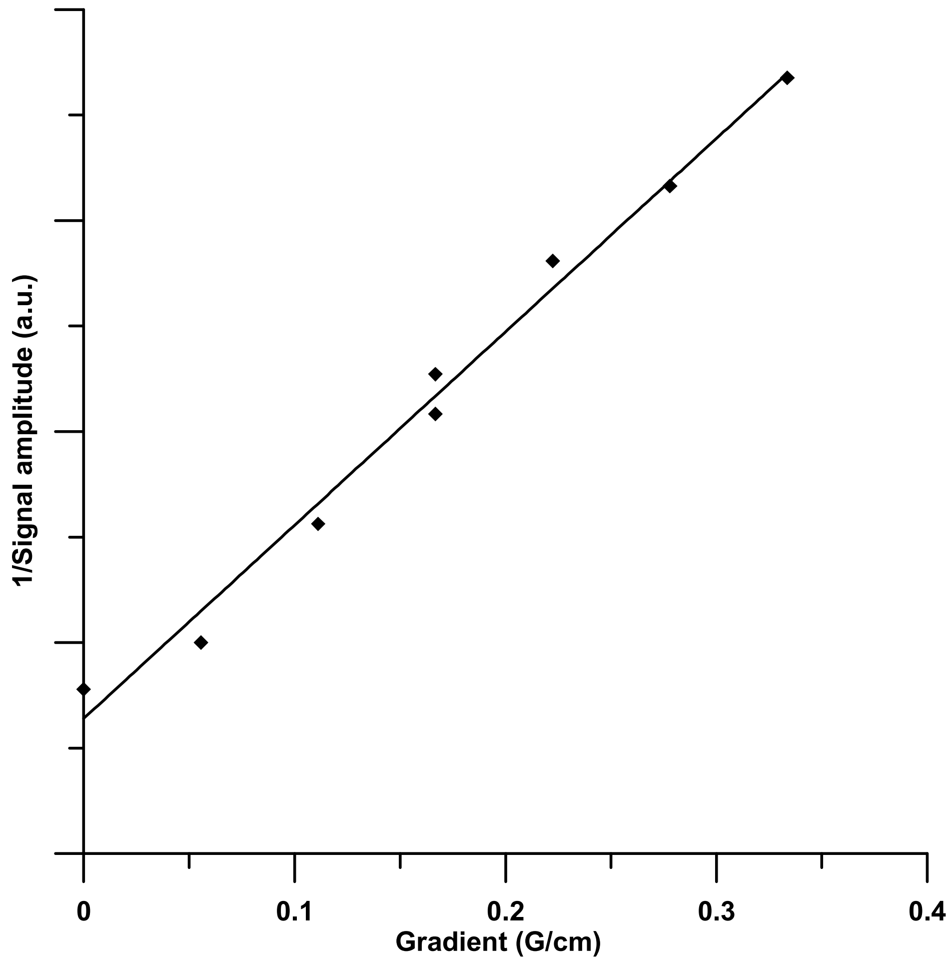

Dependence of the reciprocal of the signal amplitude on gradient.

The solid line shows the linear fit.

Maximum Entropy Image Reconstruction

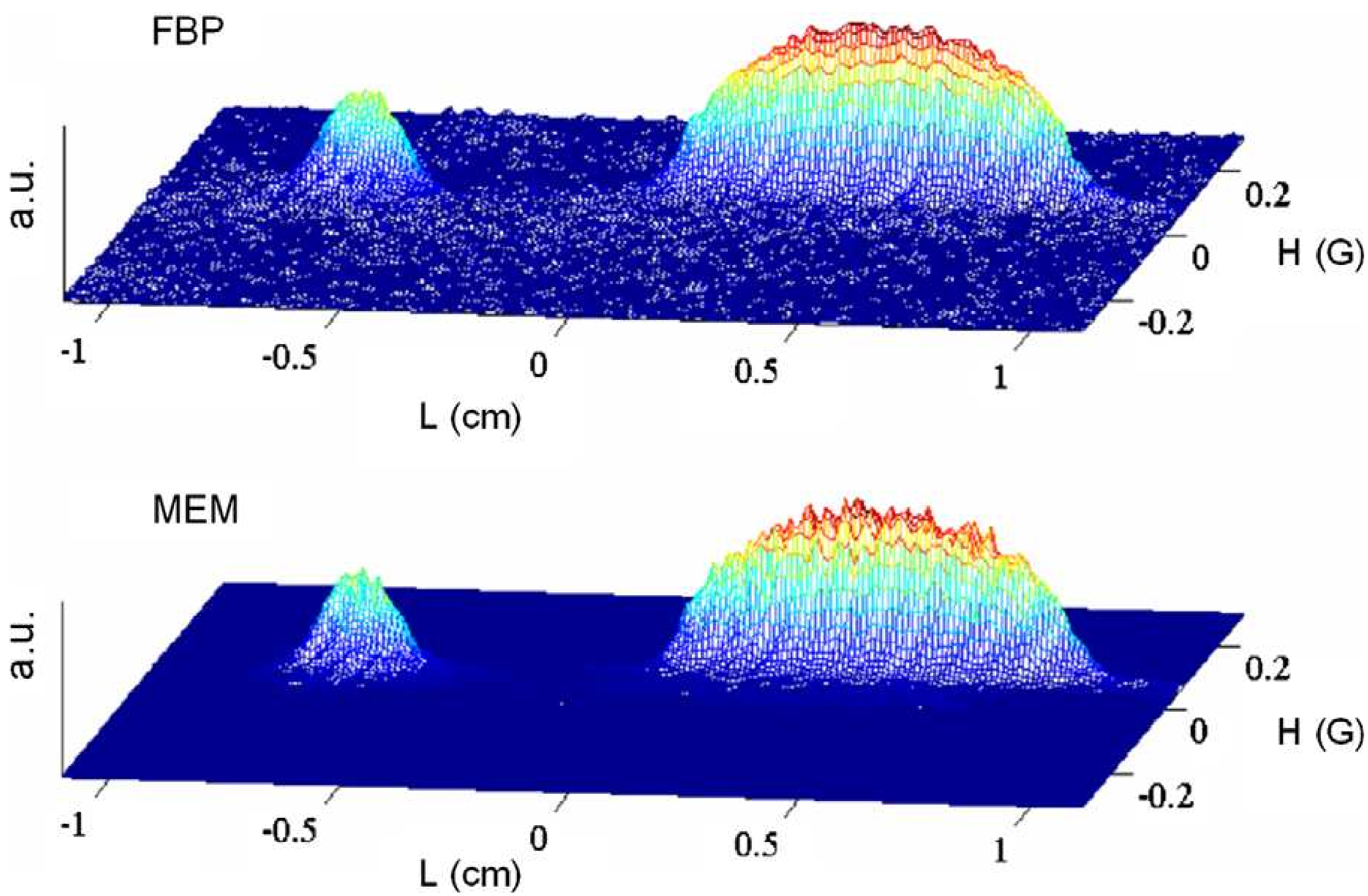

LiPc trityl-CD_3

Each of the 60 projections was averaged 5000 times with scan frequencies of 1 to 8 kHz and a scan rate of 13.9 kG/s.

A Hamming filter was used in conjunction with FBP.

No filtering was used for reconstruction by Cambridge MEM algorithm

2D spectral-spatial image of three 2 mm i.d. tubes of LiPc filled with 2%, 0%, 2% oxygen gas.
The image was reconstructed by FBP from 32 projections.

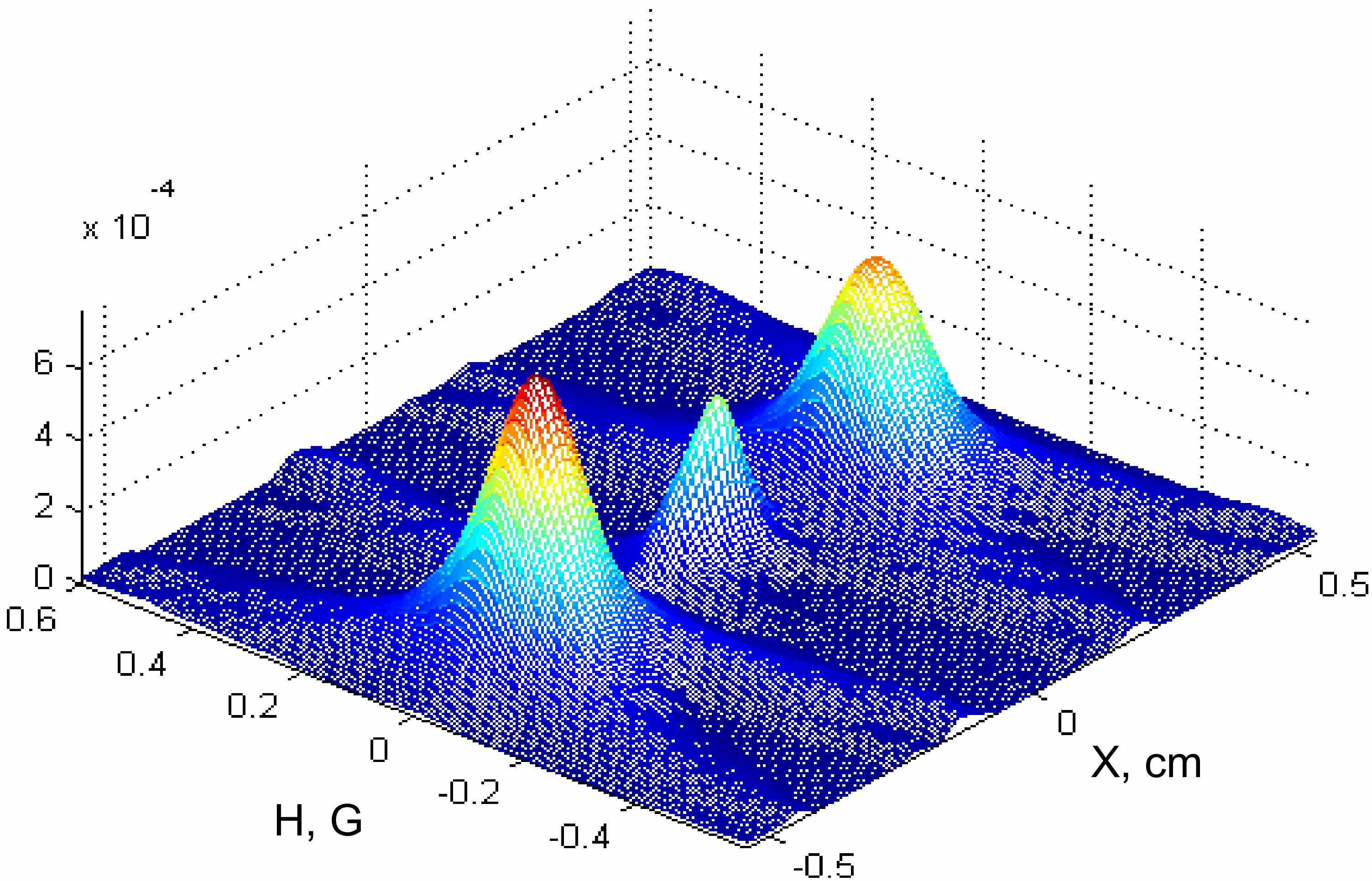

New image reconstruction approach.

Assuming one species with variable linewidth, spatial distribution a and variable linewidths γ are optimized, with Tikhonov regularization, to minimize discrepancy between calculated and experimental projections.

$$[\hat{\mathbf{a}}, \hat{\boldsymbol{\gamma}}] = \arg\min_{\mathbf{a},\boldsymbol{\gamma}} \left\{ \left\| \mathbf{RI}(\mathbf{a},\boldsymbol{\gamma}) - \mathbf{D} \right\|_2^2 + \lambda_1 \left\| \mathbf{La} \right\|_2^2 + \lambda_2 \left\| \mathbf{L}\boldsymbol{\gamma} \right\|_2^2 \right\}$$

Here $\lambda_{1,2}$ are regularization parameters to smooth reconstructed image I, R – Radon transform, D - data, and L – discrete derivative operator

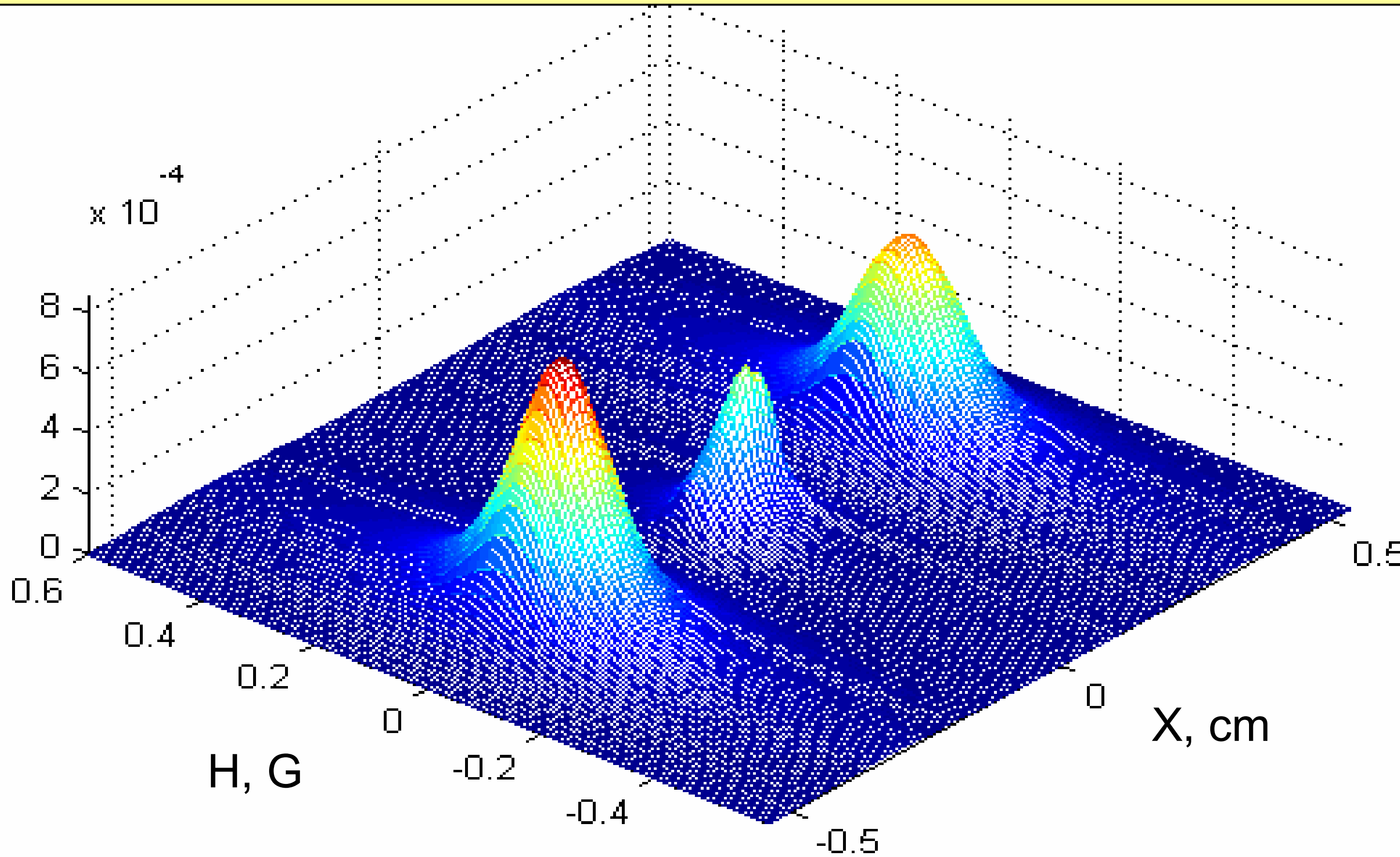

2D spectral-spatial image of two 3 mm i.d. of 0.5 mM trityl-CD_3. To broaden the line the viscosity in one tube was higher.

The image was reconstructed by FBP.

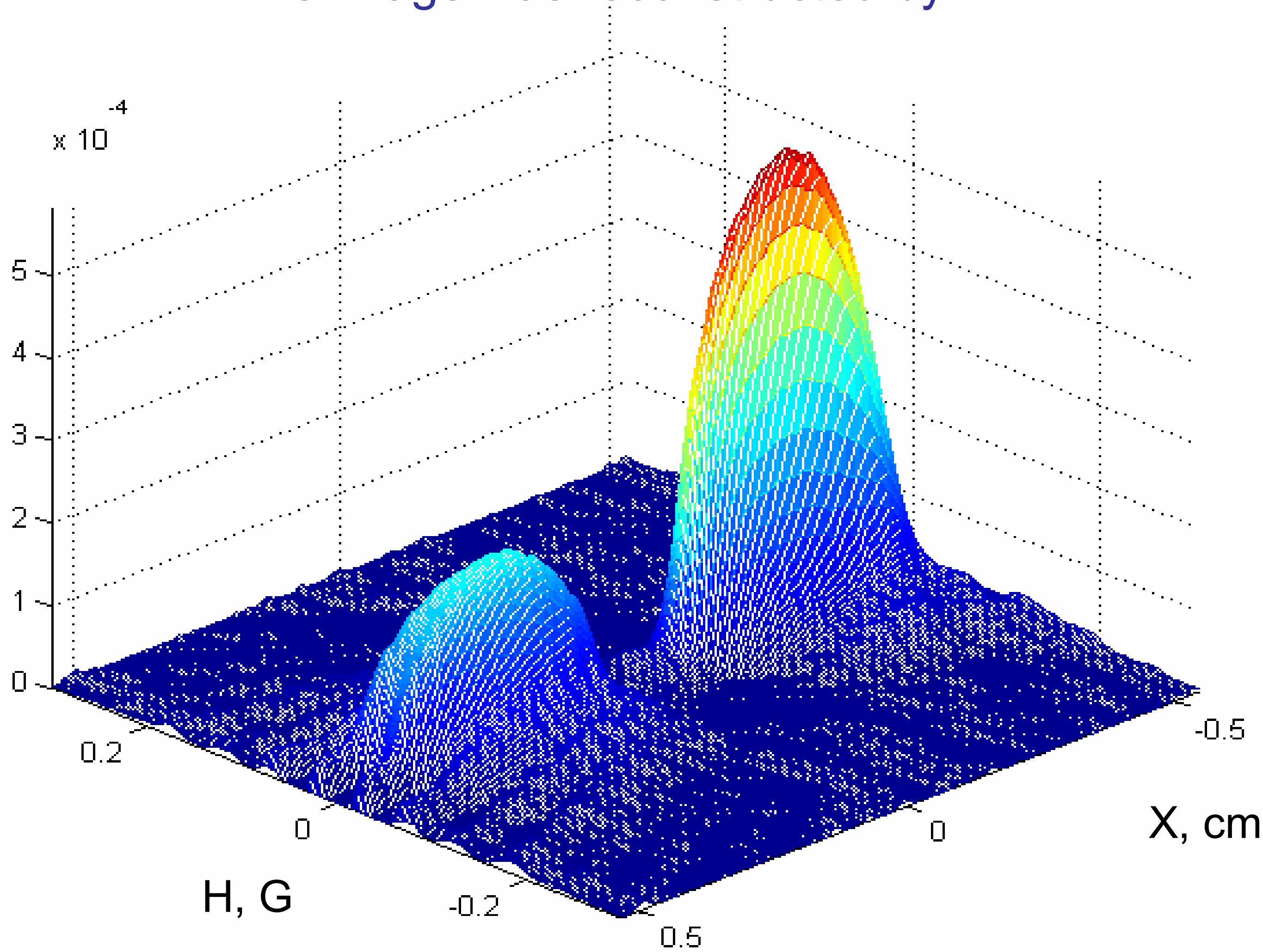

2D spectral-spatial image of two 3 mm i.d. tubes of 0.5 mM trityl-CD_3 radical. To broaden the line the viscosity in one tube was higher.

The image was reconstructed by means of FBP with each spectral slice fitted with an analytical lineshape function.

Note the well-resolved ^{13}C sidebands in the low-viscosity sample.

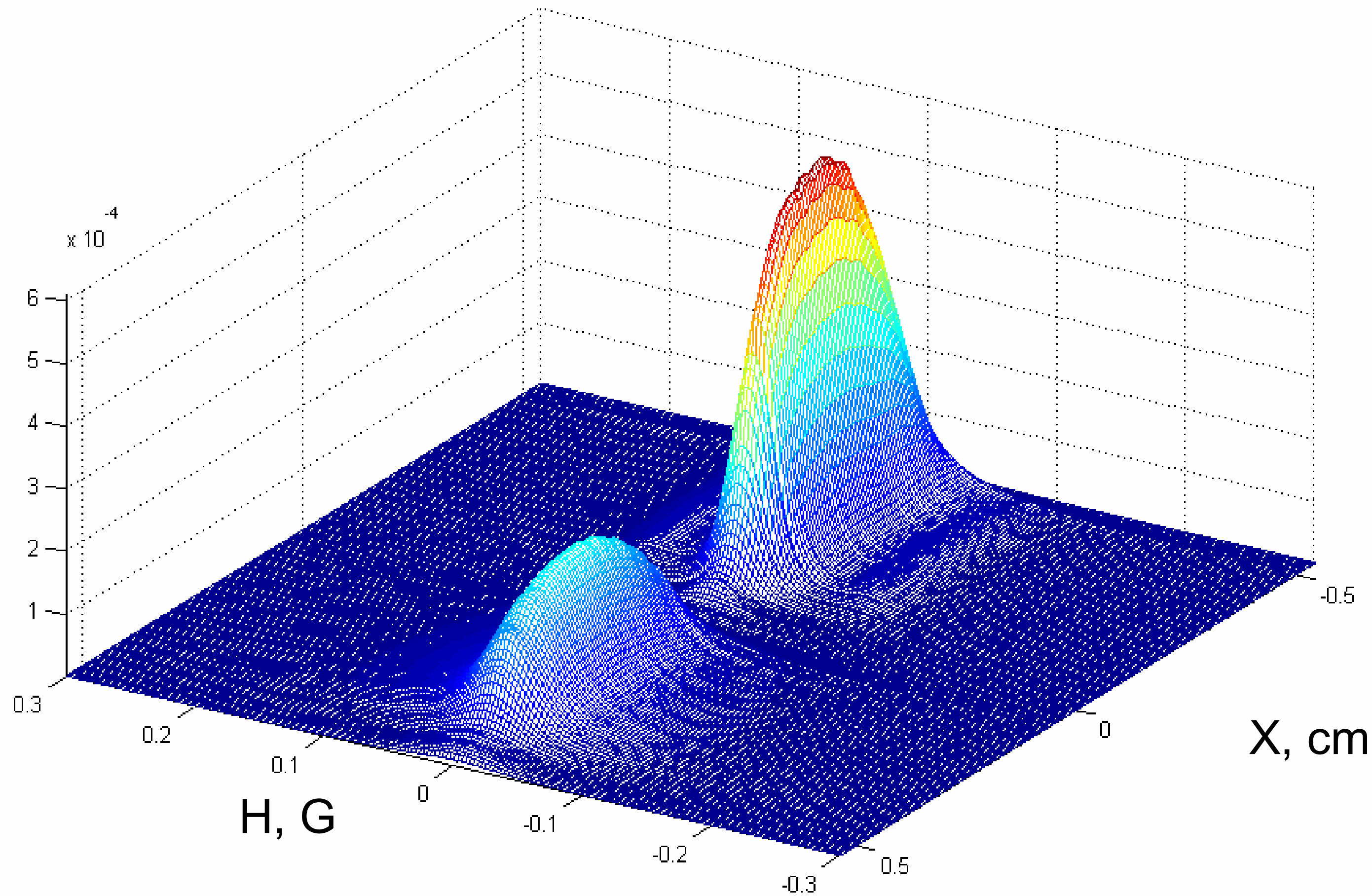

Surface coil resonator
quadrature loop/butterfly both at 250 MHz
ca. 35 dB isolation

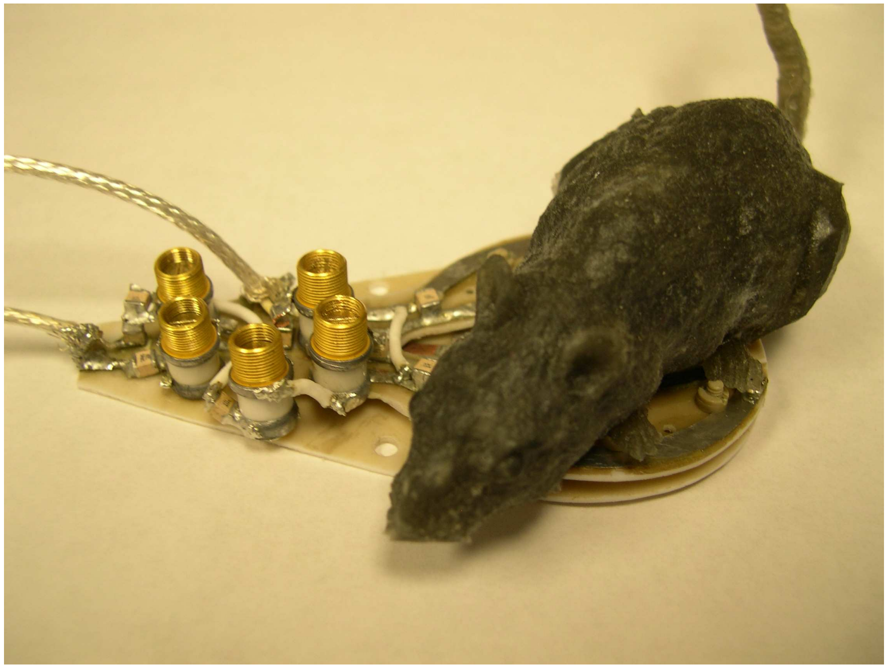

Nitroxyl Radical Spectra Using A Surface Coil

CW Compared with Rapid Scan

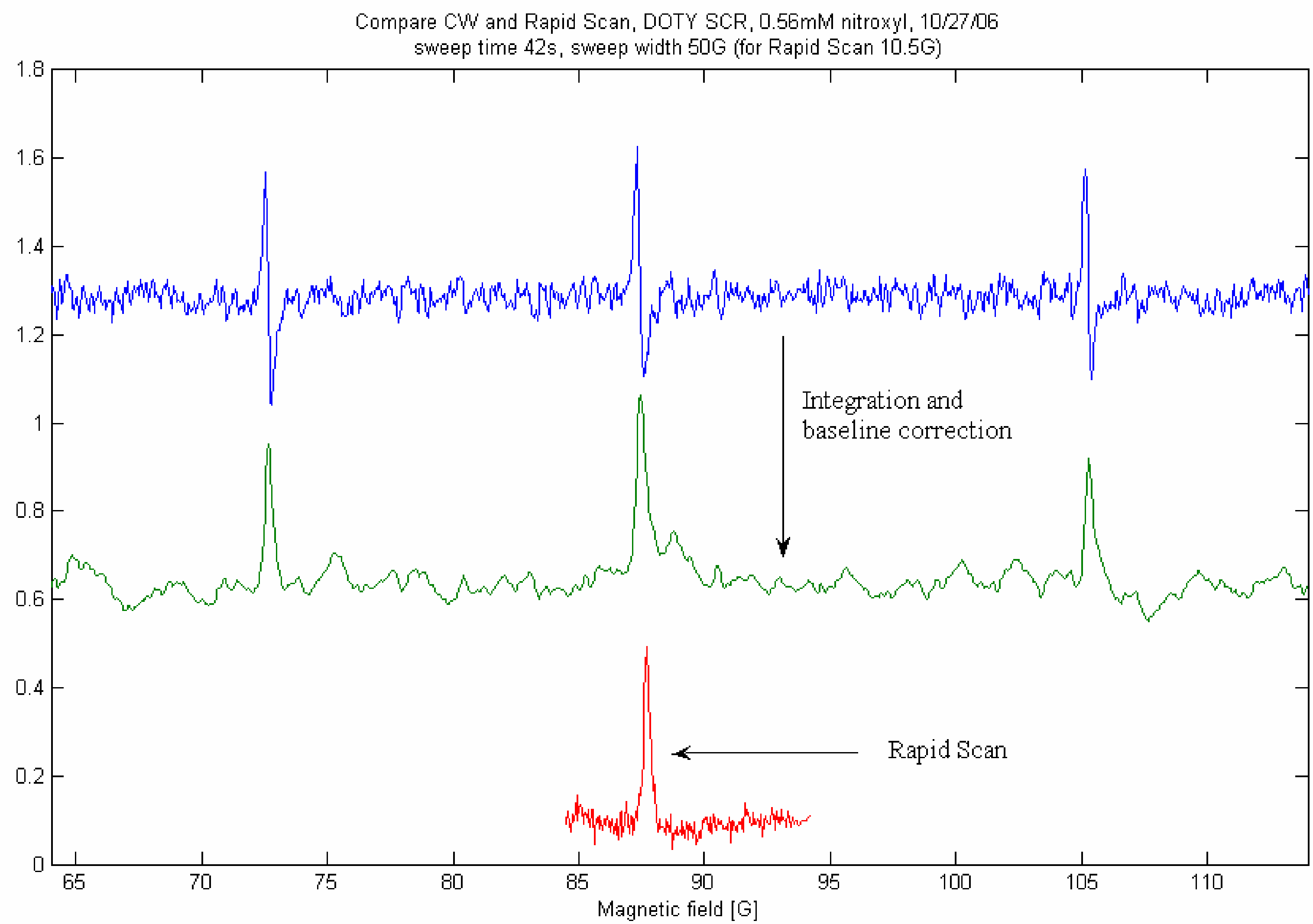

RF Source

- Source noise can be important in CW and rapid scan EPR, and for pulsed saturation-recovery EPR.
- We modeled the effect of source noise and concluded that for the large detection bandwidth we used in rapid scan EPR the Fluke 6080A source was decreasing S/N.
- A custom Wenzel 250 MHz fixed-frequency source (doubled 125 MHz crystal) improved S/N by 8 dB (factor of 2.5)

Field or frequency scan?

- At low fields used for in vivo imaging, the resonator bandwidth necessitates using magnetic field scans.
- At high frequencies (e.g., W-band) the resonator band width is sufficient to facilitate rapid frequency scans at constant field, yielding similar information.

New ideas result in new enabling technologies.

The new triangle scan driver will produce larger, more linear scans, and will implement a field center step for baseline subtraction.

Applications of Rapid Scan EPR

- In vivo imaging
- Oximetry
- Transient paramagnetic species
- Time-dependent biological processes
- Fundamental spin relaxation phenomena